

# Virtual Constraint Generators for Motion Control of Robots with Degree of Underactuation One

Rein Otsason<sup>a</sup>, Manfredi Maggiore<sup>a</sup>

<sup>a</sup>*Department of Electrical and Computer Engineering, University of Toronto  
10 King's College Road, Toronto, ON, M5S 3G4, Canada*

---

## Abstract

Virtual holonomic constraints (VHCs) are relations among the configuration variables of a mechanical control system that can be rendered invariant via feedback. A regular VHC is a VHC with the property that the accelerations imparted by the control forces are everywhere transverse to the constraint surface. This paper proposes a methodology for the design of regular VHCs for mechanical systems with degree of underactuation one based on the notion of a *virtual constraint generator*, a control system on the configuration manifold of the mechanical system whose orbits are all the regular VHCs for the mechanical system. Designing a regular VHC corresponds to designing controllers for the virtual constraint generator. We show how to design regular VHCs inducing two kinds of motions for the constrained dynamics: traversal of the VHC in one direction or oscillation back and forth along the VHC. We propose an optimal control problem for the virtual constraint generator whose solutions are regular VHCs inducing the kind of motions just described and, at the same time, meeting geometric requirements such as obstacle avoidance. We demonstrate the utility of our technique by designing a constraint for an overhead crane making the trolley move from left to right with bounded speed while ensuring that the cable angle remains within fixed limits, and a constraint for a cart-acrobot making the cart oscillate back and forth underneath an obstacle placed overhead while ensuring that the acrobot avoids the obstacle and remains as close as possible to being in the upright position.

---

## 1 Introduction

Virtual holonomic constraints (VHCs) have emerged over recent years as a powerful new tool for motion control of robots. From their initial application to the control of bipedal robots in [10], VHCs have been used to address a number of different complex motion control tasks, including path-following for a PVTOL aircraft [7], designing repetitive motions for the Furuta pendulum [27], and controlling snake robots [21]. The accumulated evidence of this work is that VHCs are a powerful alternative to the classical reference tracking framework for motion control of complex robotic systems, furnishing controllers which can be more robust than the classical options.

Applications to bipedal robots have focussed on designing constraints such that the *hybrid zero dynamics* possess a stable limit cycle. Crucially, the repeated impacts

and associated transitions of the robot at every footfall provide the key stabilizing effect. Outside of the context of bipedal locomotion, the focus of research on virtual constraints has been on control techniques to stabilize particular orbits arising from a constraint, as a substitute for this natural stabilizing action. Work on this front has included [29] and [28], which use virtual constraints to discover candidate periodic orbits and then provide a constructive procedure to stabilize those orbits, and [20], which uses a dynamic family of constraints to stabilize a particular orbit of a nominal constraint. While some of the mentioned work provides more or less systematic methods for designing constraints for specific systems, none provides a general, constructive method to design the constraint itself, which is necessarily prior to stabilizing any of its orbits.

This important constraint design process has been best explored in the context of bipedal locomotion. The earliest constraints for bipedal locomotion were simple and designed through intuition [10], but as the robots which constraints were being applied to increased in complexity, so did the methods used to design them. In [30], Bézier polynomials were first used to parametrize the constraints. Designing the constraint was then transformed into a parameter optimization problem, an ap-

---

*Email addresses:* rein.otsason@mail.utoronto.ca (Rein Otsason), maggiore@ece.utoronto.ca (Manfredi Maggiore).

<sup>1</sup> Parts of this paper were presented at the 2019 IEEE Conference on Decision and Control [22]. R. Otsason and M. Maggiore were supported by the Natural Sciences and Engineering Research Council (NSERC) of Canada.

proach which was explored and extended in [31,11,4]. More recent work has retained the use of Bézier polynomials to parametrize the constraints, but has treated constraint design as an optimal control problem for the robot using direct collocation [14,12,13]. Other work has exploited machine learning techniques in order to generate new constraints from families of existing ones [8], or to learn a representation of a constraint given a selection of open-loop gaits corresponding to the desired behaviour [9]. Besides being specialized to the particular requirements of bipedal robots, most of the approaches just described share two key features in common. The first is the use of Bézier polynomials to parametrize the constraints. The second is the reliance on the full dynamics in the *state space* of the robot in order to design the constraint to achieve a particular motion task. In contrast, the approach to constraint design proposed in this paper relies on a control system defined on the *configuration space* of the robot.

We can situate the constraint design problem in the broader context of motion planning for underactuated robots. Let  $\sigma : \mathbb{R} \rightarrow \mathcal{Q}$  be a path in the configuration space of a robot. For a fully actuated robot, it is possible to traverse this path at any speed. That is, for any time parametrization  $s : \mathbb{R} \rightarrow \mathbb{R}$ ,  $q(t) = \sigma(s(t))$  is a solution of the equations of motion for a suitable control  $\tau(t)$ . In this sense the problem of *trajectory planning* is entirely decoupled from *path planning*, and indeed this decoupling has been exploited by several different motion planning techniques (see, for example, [15,1,25,24]). For a robot with  $n$  degrees of freedom and  $m < n$  actuators, by contrast, the time parameterization must satisfy the vector differential equation [2]

$$a(s)\ddot{s} + b(s)\dot{s}^2 + c(s) = 0, \quad (1)$$

where the functions  $a, b, c : \mathbb{R} \rightarrow \mathbb{R}^{n-m}$  depend on the path  $\sigma$ . For a path  $q = \sigma(s)$ , the solutions of (1) give all possible time parametrizations  $s(t)$  that the robot can execute, and generally it may happen that (1) has no solutions, or solutions that do not conform with the design requirements of the motion control problem one is seeking to solve. Designing a *trajectory* for an underactuated system is thus inescapably linked with designing the *path*. This is one of the central difficulties of underactuated robotics.

Several different approaches have been proposed to handle this difficulty. In [2], *decoupling vector fields* were used to design paths so that the terms  $a$ ,  $b$ , and  $c$  are all zero, such that the path can be traversed at any speed, just as in the fully actuated case. Unfortunately, this approach is only applicable to systems with no potential.

More computationally driven approaches simply lift the problem to the state space (so called *kinodynamic* motion planning), and solve the motion planning using one

of many different algorithms, most popularly the randomized approach of [16] and its descendants. This approach generates time-dependent trajectories that are to be used as reference signals for asymptotic tracking. Representing desired robot behaviours in terms of timed reference signals is problematic in motion control applications such as robot locomotion where imposing a timing on the feedback loop leads to an inherent lack of robustness in the face of disturbances (see, for example, the discussion in [3] and [31, Section 1.4]). Additionally, the numerical methods used in kinodynamic motion planning do not necessarily produce trajectories that can be stabilized via feedback. Further, these algorithms do not lend themselves to a theoretical analysis offering guarantees that the generated solutions meet the requirements of the problem. Finally, when the goal is to design periodic trajectories associated to a repetitive behaviour, finding closed orbits of a large system of differential equations is a notoriously hard numerical problem.

In contrast to kinodynamic motion planning, for robots with underactuation degree one virtual constraints represent motions as paths in the configuration manifold, without imposing any timing on the feedback loop. The problem of inducing repetitive motions is greatly simplified when using virtual constraints, and indeed this problem is at the core of the papers [29,26]. In [29], a candidate path in the form of a virtual constraint was considered, and a method was devised to stabilize a periodic solution of (1), provided that such a solution exists and is known. Soon after, [26] provided a sufficient condition for the existence of such a periodic orbit, and used this to design constraints for the cart-pendulum, but did not provide a general constructive procedure for generating paths (virtual constraints) satisfying this condition. One of the contributions of this paper is to provide just such a constructive procedure.

To summarize, path planning and trajectory planning are inextricably linked for underactuated robots: the geometry of a path that the robot is to follow in the *configuration space* determines the kind of trajectories in the *state space* that the robot is able to track. To date there has been no systematic attempt at designing paths in the configuration space inducing desired qualitative properties for the trajectories that the robot can produce along these paths. This paper initiates such an investigation. We note that the approach we develop here is independent of, and indeed complementary to, the various techniques which have been developed to stabilize constraints or particular trajectories along them. The constraints designed here may be stabilized by various methods, including but not limited to feedback linearization and sliding-mode control; in this regard the problem of designing constraints inducing certain dynamics is similar to the problem of designing an appropriate sliding surface in sliding-mode control.

**Contributions of this paper.** For robots with a single degree of underactuation, this paper makes three contributions. First, in Section 3 we introduce a tool we call the *virtual constraint generator* (VCG), a virtual control system on the *configuration space* of the robot with the property that its solutions are *all* regular VHCs for the robot (regular VHCs are reviewed in Section 2).

The second contribution, in Section 5, is to show precisely which properties a VHC curve must possess in order that the motion of the robot along this curve corresponds to one of these two desired behaviours: either the robot’s configuration traverses the entire curve in one direction, or it oscillates back and forth along the curve. We convert these requirements into control specifications for the VCG and show that searching for a regular VHC inducing one of the two foregoing behaviours corresponds to designing a virtual controller for the VCG meeting one of two control specifications which we call *dynamic specifications*. This is an important conceptual transition: *constraint design* problems are turned into *control design* problems for the VCG. There are additional *geometric specifications* to be met, and these correspond to the standard objectives of path planning. Among these are to ensure that the VHC curve be contained in a safe set (obstacle avoidance) and that certain quantities increase monotonically along the curve (monotonicity).

The final contribution of this paper is the formulation, in Section 6, of an optimal control problem for the VCG encompassing both the dynamic and geometric specifications. In contrast with other constraint design approaches reviewed earlier, this optimal control problem is posed on the *configuration space* of the robot.

The ideas of this paper are illustrated by means of two motion control problems, introduced in Section 4 and solved in Sections 7 and 8. The first problem concerns an overhead crane. The objective is to make the trolley move from left to right with bounded speed while ensuring that the cable angle remains within fixed limits. The second problem concerns an acrobat on a cart. Here the objective is to make the cart oscillate back and forth underneath an obstacle placed overhead while ensuring that the acrobat avoids the obstacle and remains as close as possible to being in the upright position.

**Notation.** We denote the  $i$ -th standard basis vector of  $\mathbb{R}^n$  by  $\mathbf{e}_i$ . If  $v \in \mathbb{R}^n$ , we denote by  $v_i$  the  $i$ -th component of  $v$ . Similarly, for a vector-valued function  $f$ ,  $f_i$  denotes the  $i$ -th component of  $f$ . For  $T > 0$  and  $x \in \mathbb{R}$ , we denote by  $[x]_T$  the quantity  $x$  modulo  $T$ , and by  $[\mathbb{R}]_T$  the set of real numbers modulo  $T$ . If  $M$  be a smooth manifold and  $x \in M$ , we denote by  $T_x M$  the tangent space to  $M$  at  $x$ , and by  $TM$  the tangent bundle of  $M$ . If  $f : \mathbb{R}^n \rightarrow \mathbb{R}^m$  is a smooth function and  $x \in \mathbb{R}^n$ , then by  $df_x$  we denote the Jacobian matrix of  $f$  at  $x$ . If  $g_1, \dots, g_k$  is a collection of vector fields on  $\mathbb{R}^n$ , and  $f : \mathbb{R}^n \rightarrow \mathbb{R}^m$  is a smooth function, then  $L_g f : \mathbb{R}^n \rightarrow \mathbb{R}^{m \times k}$  denotes the function

$x \mapsto [df_x g_1(x) \cdots df_x g_k(x)]$ . We denote by  $\text{GL}(n; \mathbb{R})$  the set of invertible  $n \times n$  real matrices. Finally, we use dots to denote differentiation with respect to time and primes to denote differentiation with respect to the constraint parameter  $s$ .

## 2 Background on Virtual Holonomic Constraints

In this section we review the basic setup of mechanical systems and virtual holonomic constraints. This material can be found in the references [18–20,5]. Let  $q = (q_1, \dots, q_n)$  be generalized coordinates for a simple mechanical system. Each coordinate  $q_i$  is either an element of  $\mathbb{R}$ , corresponding to a translational degree of freedom, or an element of  $[\mathbb{R}]_{2\pi}$ , corresponding to a rotational degree of freedom. The configuration manifold  $\mathcal{Q}$  is thus a generalized cylinder. The equations of motion for a simple mechanical control system with  $m$  inputs are

$$D(q)\ddot{q} + C(q, \dot{q})\dot{q} + \nabla P(q) = B(q)\tau, \quad (2)$$

where  $D : \mathcal{Q} \rightarrow \mathbb{R}^{n \times n}$  is the mass matrix, assumed to be everywhere symmetric and positive definite,  $C : T\mathcal{Q} \rightarrow \mathbb{R}^{n \times n}$  is the Coriolis matrix,  $P : \mathcal{Q} \rightarrow \mathbb{R}$  is the potential,  $B : \mathcal{Q} \rightarrow \mathbb{R}^{n \times m}$  is the input matrix, and  $\tau = (\tau_1, \dots, \tau_m)$  is the vector of control forces. If  $m < n$ , then the system is *underactuated*, and  $n - m$  is the *degree of underactuation*. We assume that the matrix  $B(q)$  has full rank for all  $q \in \mathcal{Q}$ . We also assume that  $B$  has a smooth left annihilator  $B^\perp : \mathcal{Q} \rightarrow \mathbb{R}^{(n-m) \times n}$ , that is, a function  $B^\perp$  such that  $B^\perp(q)$  is full rank and  $B^\perp(q)B(q) = 0$  for all  $q \in \mathcal{Q}$ .

In this paper, a *virtual holonomic constraint* (VHC) for the system (2) is an embedded curve  $\mathcal{C} \subset \mathcal{Q}$  satisfying the following *regularity* condition: for each  $q \in \mathcal{Q}$ ,

$$T_q \mathcal{C} \oplus \text{Im}(D^{-1}(q)B(q)) = T_q \mathcal{Q}. \quad (3)$$

This regularity condition has an intuitive physical meaning. Considering the equations of motion (2), at each point  $q \in \mathcal{Q}$  the subspace  $\text{Im}(D^{-1}(q)B(q))$  is the vector space of directions in which we can accelerate using our control inputs. The condition in (3) requires that at each point of the constraint curve  $\mathcal{C}$ , this subspace be transverse to the curve, so that accelerations can be applied to drive the configuration  $q(t)$  onto the constraint and keep it there. Some other approaches in the literature (see [29,28] and related work) do not require regular constraints, since requiring regularity implies a possibility of missing potentially desirable trajectories. But, as we show in a moment, regularity brings about two benefits. First, it guarantees that the constraint manifold itself is *stabilizable*, and not just one of the trajectories on it. Second, it guarantees the existence of well-defined constrained dynamics, substantially easing analysis, a feature that will be put to use throughout the rest of this paper.

The tangent bundle  $\Gamma := T\mathcal{C} = \{(q, \dot{q}) \in T\mathcal{Q} : q \in \mathcal{C}, \dot{q} \in T_q\mathcal{C}\}$  is called the *constraint manifold*, and the regularity property (3) guarantees that there is a unique smooth feedback  $\tau : \Gamma \rightarrow \mathbb{R}^{n-1}$  rendering  $\Gamma$  invariant. This fact implies that there are uniquely defined constrained dynamics on  $\Gamma$ , as we shall see in a moment.

A VHC admits two representations: implicit and parametric. In the *implicit representation*,  $\mathcal{C}$  is expressed as  $\mathcal{C} = \{q \in \mathcal{Q} : h(q) = 0\}$ , where  $h : \mathcal{Q} \rightarrow \mathbb{R}^{n-1}$  is a smooth function whose Jacobian is nonvanishing at all  $q \in h^{-1}(0)$ . In this case, the regularity condition (3) is equivalent to requiring system (2) with output  $e = h(q)$  to have well-defined vector relative degree  $\{2, \dots, 2\}$  everywhere on  $\Gamma$  (which amounts to the invertibility of the matrix  $dh_q D^{-1}(q)B(q)$  at all  $q \in h^{-1}(0)$ ), and the constraint manifold  $\Gamma$  is the zero dynamics manifold associated with the output  $e = h(q)$ . The implicit representation is used to design feedbacks that asymptotically stabilize  $\Gamma$  (and therefore asymptotically enforce the constraint) through input-output linearization<sup>2</sup>.

In the *parametric representation*,  $\mathcal{C}$  is expressed as a parametric curve  $q = \sigma(s)$ , where  $\sigma : \mathbb{I} \rightarrow \mathcal{Q}$  is a  $C^2$  function that is a diffeomorphism onto its image, with domain  $\mathbb{I} = \mathbb{R}$  if the curve is not closed, or  $\mathbb{I} = [\mathbb{R}]_T$ , for some  $T > 0$ , if the curve is closed. For closed curves, one typically starts with a  $T$ -periodic parametrization  $\hat{\sigma} : \mathbb{R} \rightarrow \mathcal{Q}$ , and defines  $\sigma : [\mathbb{R}]_T \rightarrow \mathcal{Q}$  to be the unique  $C^2$  function satisfying the identity  $\hat{\sigma}(s) = \sigma([s]_T)$ . This corresponds to identifying points in the domain of  $\hat{\sigma}$  whose difference is an integer multiple of  $T$ . For parametric VHCs, the regularity condition (3) becomes

$$\text{span}(\sigma'(s)) \oplus \text{Im}(D^{-1}(\sigma(s))B(\sigma(s))) = T_{\sigma(s)}\mathcal{Q} \quad (4)$$

for all  $s \in \mathbb{I}$ . In the above, we have used primes to denote differentiation with respect to the constraint parameter  $s$ . We shall adopt this convention for the rest of this paper, while reserving dots to denote differentiation with respect to time  $t$ .

While implicit representations are useful for control design, parametric representations are useful to determine the dynamics on the constraint manifold. Specifically, substituting  $q = \sigma(s(t))$  and its time derivatives in (2) and premultiplying both sides of the equation by  $B^\perp$ ,

one can solve for  $\ddot{s}$  and obtain (see [19,20,29,32])

$$\ddot{s} = \Psi_1(s) + \Psi_2(s)\dot{s}^2, \quad (s, \dot{s}) \in \mathbb{I} \times \mathbb{R}, \quad (5)$$

$$\Psi_1(s) = - \left. \frac{B^\perp \nabla P}{B^\perp D\sigma'(s)} \right|_{q=\sigma(s)}, \quad (6)$$

$$\Psi_2(s) = - \left. \frac{B^\perp (D\sigma'' + C(\sigma, \sigma'))}{B^\perp D\sigma'(s)} \right|_{q=\sigma(s)}. \quad (7)$$

Any solution  $(q(t), \dot{q}(t))$  of (2) which is entirely contained in  $\Gamma$  has the form  $(q(t), \dot{q}(t)) = \Phi(s(t), \dot{s}(t)) := (\sigma(s(t)), \sigma'(s(t))\dot{s}(t))$ , where the map  $\Phi : T\mathbb{I} \rightarrow T\mathcal{Q}$  is a diffeomorphism onto  $\Gamma$ , and the pair  $(s(t), \dot{s}(t))$  is a solution of (5). For this reason, we refer to (5) as the *constrained dynamics*. The denominators involved in the above quantities are guaranteed to be non-zero by the regularity condition (4).

While in classical mechanics the dynamics of a mechanical system subject to a holonomic constraint are always Euler-Lagrange, the same is not necessarily true for a virtual holonomic constraint. In [19], it is shown that a sufficient condition for the constrained dynamics to be Lagrangian is that  $\mathbb{I} = \mathbb{R}$ , i.e. that the constraint is an open curve in  $\mathcal{Q}$ . If the dynamics on a VHC are Euler-Lagrange, then the associated Lagrangian is

$$L = \frac{1}{2}M(s)\dot{s}^2 - V(s), \quad (8)$$

where  $M(s)$  and  $V$  are the *virtual mass* and *virtual potential*, defined as

$$M(s) = \exp\left(-2 \int_0^s \Psi_2(\tau) d\tau\right), \quad (9a)$$

$$V(s) = - \int_0^s \Psi_1(\tau)M(\tau) d\tau. \quad (9b)$$

When the constrained dynamics (5) are Euler-Lagrange, they possess a first integral

$$E(s, \dot{s}) = \frac{1}{2}M(s)\dot{s}^2 + V(s), \quad (10)$$

which in analogy with mechanical systems we call the *total virtual energy*. See also [29].

### 3 Virtual Constraint Generator

In this paper a central goal is the systematic design and generation of virtual holonomic constraints. The tool we shall use for this task is the *virtual constraint generator* (VCG), which was introduced in [22], and generalized earlier work in [6]. A virtual constraint generator, as we define it here, is a virtual control system on the configuration manifold with the property that every possible

<sup>2</sup> Provided that the function  $(q, \dot{q}) \mapsto (h(q), h_q \dot{q})$  is lower and upper bounded by a class- $\mathcal{K}$  function of the point-to-set distance of  $(q, \dot{q})$  to  $\Gamma$ , see [18].

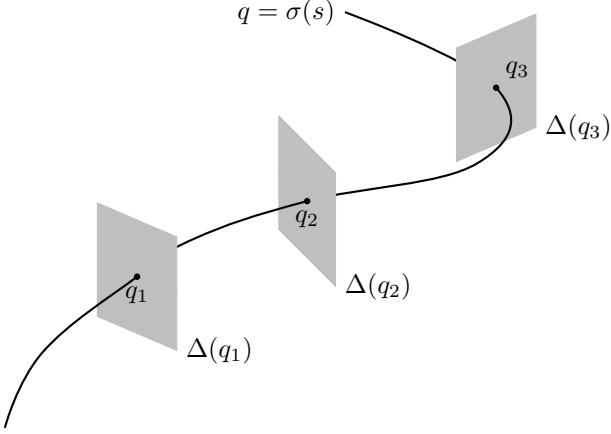


Fig. 1. A parametric VHC must be everywhere transverse to  $\Delta(q)$  in order to be regular

parametric VHC is a solution of the generator for some virtual control input.

We begin by constructing the VCG from simple considerations stemming from the properties of regular VHCs discussed in the preceding section. Recall the transversality requirement (4). Let  $\Delta(q) = \text{Im}(D^{-1}(q)B(q))$ . The distribution  $\Delta(q)$  assigns to each point  $q \in \mathcal{Q}$  an  $(n-1)$ -dimensional hyperplane. The transversality requirement (4) means that a parametric VHC  $q = \sigma(s)$  must cross these hyperplanes at each point. Generating VHCs, then, is equivalent to finding all curves that are everywhere transverse to the distribution  $\Delta(q)$ . Figure 1 illustrates this situation.

Consider a vector field  $f : \mathcal{Q} \rightarrow T\mathcal{Q}$  such that  $f$  is transverse to  $\Delta(q)$  for all  $q \in \mathcal{Q}$ . For instance, one could choose  $f(q) = (B^\perp(q))^\top$ . Let  $q = \sigma(s)$  be an integral curve of  $f$ . Then  $q = \sigma(s)$  is a parametric VHC, since by construction for all  $s$  the tangent vector  $\sigma'(s)$  satisfies

$$\text{span}(\sigma'(s)) \oplus \Delta(q) = T_{\sigma(s)}\mathcal{Q}.$$

All integral curves of  $f$  are parametric VHCs, but  $f$  alone cannot produce all possible VHCs. Let  $g : \mathcal{Q} \rightarrow T\mathcal{Q}$  be a smooth vector field such that  $g(q) \in \Delta(q)$  for all  $q \in \mathcal{Q}$ . Then the vector field  $f + g$  is also everywhere transverse to  $\Delta$ , and so every integral curve of  $f + g$  is also a parametric VHC. More generally, let  $g : \mathcal{Q} \rightarrow \mathbb{R}^{n \times (n-1)}$  be any matrix-valued function such that  $\text{Im}(g(q)) = \Delta(q)$  for all  $q \in \mathcal{Q}$ . An obvious choice would be  $g(q) = D^{-1}(q)B(q)$ . Then for all  $u \in \mathbb{R}^{n-1}$ ,  $g(q)u \in \Delta(q)$ . This motivates the following definition of the virtual constraint generator.

**Definition 1.** Consider a simple mechanical system (2) with degree of underactuation 1 and the smooth distribution on  $\mathcal{Q}$  given by  $\Delta(q) = \text{Im}(D^{-1}(q)B(q))$ . A *virtual constraint generator* (VCG) for the system is a control

system on  $\mathcal{Q}$  with  $n-1$  control inputs,

$$\frac{dq}{ds} = f(q) + g(q)u, \quad (11)$$

where  $f$  is any smooth vector field such that for all  $q \in \mathcal{Q}$ ,

$$\text{span}(f) \oplus \Delta(q) = T_q\mathcal{Q}, \quad (12)$$

and  $g : \mathcal{Q} \rightarrow \mathbb{R}^{n \times (n-1)}$  is any smooth matrix-valued function such that  $\text{Im}(g(q)) = \Delta(q)$  for all  $q \in \mathcal{Q}$ .

Equivalently, a VCG is characterized by these two properties:

- (i) The matrix-valued function  $\mathcal{Q} \rightarrow \mathbb{R}^{n \times n}$  given by  $\begin{bmatrix} f(q) & g(q) \end{bmatrix}$  is invertible for all  $q \in \mathcal{Q}$ .
- (ii)  $\text{Im}(g(q)) = \text{Im}(D^{-1}(q)B(q))$  for all  $q \in \mathcal{Q}$ .

It is easy to establish that a virtual constraint generator always exists. The matrix  $D^{-1}(q)B(q)$  trivially satisfies the requirements for  $g$ , and the vector field  $(B^\perp(q))^\top$  satisfies the transversality requirements for  $f$ , so that

$$\frac{dq}{ds} = (B^\perp(q))^\top + D^{-1}(q)B(q)u \quad (13)$$

is a suitable choice for a VCG for any system (2) meeting our assumptions. For computational reasons, we usually choose to replace  $D^{-1}(q)$  in the above with  $\text{adj}(D(q))$ , which simply corresponds to scaling the control  $u$  by  $\det(D(q))$ . This replacement is formally justified by Proposition 3 below.

We have explicitly constructed the virtual constraint generator in such a way that any of its solutions satisfies the fundamental transversality requirement for a regular VHC. The following theorem formalizes this, and additionally establishes that *any* parametric VHC is a solution of the constraint generator for some virtual control input.

In what follows, a *reparametrization* of a parametric VHC  $\sigma : \mathbb{I} \rightarrow \mathcal{Q}$  is another parametric VHC  $\tilde{\sigma}(\tilde{s}) := \sigma(\mu(\tilde{s}))$ , where  $\mu$  is a smooth function  $\mathbb{R} \rightarrow \mathbb{R}$  if  $\mathbb{I} = \mathbb{R}$ , or  $[\mathbb{R}]_T \rightarrow [\mathbb{R}]_{T'}$ , with  $T' > 0$ , if  $\mathbb{I} = [\mathbb{R}]_T$ . Moreover,  $\mu'(\tilde{s}) \neq 0$  for all  $\tilde{s} \in \mathbb{I}$ .

For notational consistency with the notion of parametric VHC introduced in Section 2, solutions of the control system (11) will be denoted by  $\sigma(s)$ , with the convention that if  $\sigma$  is  $T$ -periodic, with  $T > 0$ , then we take its domain to be  $[\mathbb{R}]_T$ , per the construction in Section 2.

**Theorem 2.** Consider the VCG (11) and a  $C^1$  signal  $u : \mathbb{R} \rightarrow \mathbb{R}^{n-1}$  giving a globally defined solution  $\sigma : \mathbb{I} \rightarrow \mathcal{Q}$ , whose image is an embedded curve in  $\mathcal{Q}$ , where  $\mathbb{I} = \mathbb{R}$  if the curve is not closed, and  $\mathbb{I} = [\mathbb{R}]_T$ , with  $T > 0$ , if the

curve is closed. Then the curve  $q = \sigma(s)$  is a parametric VHC for system (2). Vice versa, if  $\sigma : \mathbb{I} \rightarrow \mathcal{Q}$  is such that  $q = \sigma(s)$  is a parametric VHC for system (2), then there exists a reparametrization  $\sigma \circ \mu(\tilde{s})$  that is a solution of (11) for a suitable  $C^1$  virtual control signal  $\bar{u}(\tilde{s})$ .

*Proof.* Let  $\sigma : \mathbb{I} \rightarrow \mathcal{Q}$  be a solution of (11) corresponding to a smooth virtual control signal  $\bar{u}(s)$ . For each  $s \in \mathbb{I}$ , we have  $\sigma'(s) = f(\sigma(s)) + g(\sigma(s))\bar{u}(s)$ . Since  $f$  satisfies (12), it follows that the transversality condition (4) holds, and therefore  $q = \sigma(s)$  is a VHC for (2).

Now let  $q = \sigma(s)$  be a parametric VHC so that, by definition, the transversality condition (4) holds. We need to find a smooth function  $\mu$  such that  $\mu' \neq 0$ , and a  $C^1$  virtual control signal  $\bar{u}$  such that, letting  $\tilde{\sigma} = \sigma \circ \mu$  and  $s = \mu(\tilde{s})$ , it holds that

$$\frac{d\tilde{\sigma}}{d\tilde{s}} = f(\tilde{\sigma}) + g(\tilde{\sigma})\bar{u}(\tilde{s}). \quad (14)$$

By (12), the matrix-valued function  $T(q) = [f(q) \ g(q)]$  is everywhere nonsingular. Letting  $U(s) = T^{-1}(\sigma(s))\sigma'(s)$ , we have

$$\sigma'(s) = f(\sigma(s))U_1(s) + g(\sigma(s))U_{2:n}(s),$$

where  $U_1$  is the first component of  $U$  and  $U_{2:n}$  is the vector containing the last  $n-1$  components of  $U$ . Since  $\sigma$  is  $C^2$ ,  $U$  is  $C^1$ . Moreover, since  $\sigma(s)$  satisfies (4), the function  $U_1(s)$  is nowhere zero. Let  $\mu(\tilde{s}) = \int_0^{\tilde{s}} (1/U_1(s)) ds$ . Then,  $\mu' = 1/U_1 \neq 0$ , and letting  $\tilde{\sigma}(\tilde{s}) = \sigma \circ \mu(\tilde{s})$ , we have

$$\begin{aligned} \frac{d\tilde{\sigma}}{d\tilde{s}} &= \frac{1}{U_1(\mu(\tilde{s}))} \sigma'(\mu(\tilde{s})) \\ &= f(\tilde{\sigma}(\tilde{s})) + g(\tilde{\sigma}(\tilde{s})) \frac{U_{2:n}(\mu(\tilde{s}))}{U_1(\mu(\tilde{s}))}. \end{aligned}$$

Denoting  $\bar{u}(\tilde{s}) = U_{2:n}(\mu(\tilde{s}))/U_1(\mu(\tilde{s}))$ , the function  $\tilde{\sigma}(\tilde{s})$  is  $C^1$  because  $U$  is  $C^1$  and  $U_1 \neq 0$ , and  $\bar{u}$  satisfies (14), as required.  $\square$

The preceding result guarantees that the orbits of any VCG are all possible regular VHCs for the given system. That is, any choice of VCG generates the exact same VHCs (orbits); the only thing that is different between two VCGs for a system is a possible difference in the parameterizations of the constraints they generate. This naturally leads to the following two questions: what relationships exist between all possible VCGs for a given mechanical system, and how is the reparametrization of a parametric VHC reflected in the VCG? The following two results answer these questions. The first shows that any two VCGs for the same mechanical system are related by a simple scaling of the drift vector field and a feedback

transformation. The second shows that a reparametrization of a parametric VHC is accomplished by a simultaneous scaling of the drift vector field and a reparametrization of the control. Their proofs are in Appendix A.

**Proposition 3.** *If (11) is a VCG for system (2), then all other VCGs for (2) are related to (11) via a regular feedback transformation and a nonvanishing scaling of the drift vector field  $f$ , i.e., they have the form*

$$\frac{dq}{ds} = (\alpha(q)f(q) + g(q)K_1(q)) + g(q)K_2(q)v, \quad (15)$$

where  $\alpha : \mathcal{Q} \rightarrow \mathbb{R} \setminus \{0\}$ ,  $K_1 : \mathcal{Q} \rightarrow \mathbb{R}^m$  and  $K_2 : \mathcal{Q} \rightarrow \text{GL}(n-1; \mathbb{R})$  are smooth, and  $v \in \mathbb{R}^{n-1}$  is the virtual control input.

The next result states that scaling the drift vector field of the VCG by a nonvanishing scalar-valued function corresponds to reparametrizing the VHCs generated by the VCG. Moreover, it shows that *any* reparametrization of a VHC arises from such a scaling of the drift vector field of the VCG.

**Proposition 4.** *Let  $\sigma(s)$  be a solution of the VCG (11) with input signal  $u = \bar{u}(s)$  such that the curve  $q = \sigma(s)$  is a closed embedded submanifold of  $\mathcal{Q}$ . Then, for each reparametrization  $\tilde{\sigma}(\tilde{s}) = \sigma(\mu(\tilde{s}))$ , there exists a smooth function  $\alpha : \mathcal{Q} \rightarrow \mathbb{R} \setminus \{0\}$  such that  $\tilde{\sigma}$  is a solution of the VCG*

$$\frac{dq}{d\tilde{s}} = \alpha(q)f(q) + g(q)u \quad (16)$$

with input signal  $u = \bar{u}(\mu(\tilde{s}))\mu'(\tilde{s})$ . Vice versa, for each smooth function  $\alpha : \mathcal{Q} \rightarrow \mathbb{R} \setminus \{0\}$ , there is a reparametrization  $\tilde{\sigma}(\tilde{s}) = \sigma(\mu(\tilde{s}))$  such that  $\tilde{\sigma}(\tilde{s})$  is a solution of the VCG (16) with input signal  $u = \alpha(\sigma(\mu(\tilde{s})))\bar{u}(\mu(\tilde{s}))$ , where the reparametrizing function  $\mu$  is the solution of the differential equation

$$\frac{dx}{d\tilde{s}} = \alpha(\sigma(x))$$

with initial condition  $x(0) = \mu(0)$ .

## 4 Model problems

In order to clarify the rest of our presentation, we will pause our theoretical development here to present two basic mechanical systems. We will demonstrate how to construct a VCG for each system, and then present a motion control problem for each, the solutions to which we will find in Sections 7 and 8.

### 4.1 Overhead crane

Consider a trolley of mass  $M$  that has position  $x$  along a linear track, and an attached payload that is modelled

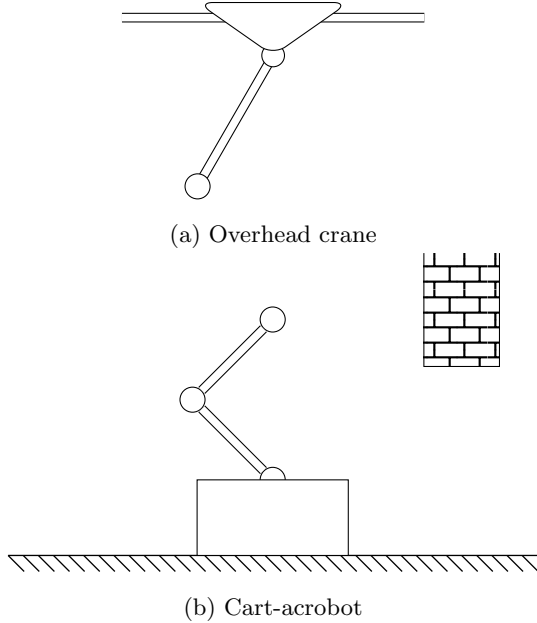


Fig. 2. Motivating examples

as a point mass  $m$  suspended from an inflexible cable of constant length  $l$ . The angle of the payload  $\theta$  is measured clockwise from the vertical. The configuration vector is  $q = (x, \theta)$ . The mass matrix is

$$D(q) = \begin{bmatrix} M + m & -ml \cos(\theta) \\ -ml \cos(\theta) & ml^2 \end{bmatrix},$$

and the potential is  $P(q) = -mgl \cos(\theta)$ . Since the cart is actuated, the input matrix is  $B(q) = \mathbf{e}_1$ . Selecting as a smooth left annihilator  $(B^\perp(q))^\top = -\mathbf{e}_2$ , and  $\text{adj}(D(q))B(q)$  as  $g$ , the VCG is

$$\frac{dq}{ds} = \begin{bmatrix} 0 \\ -1 \end{bmatrix} + \begin{bmatrix} ml^2 \\ ml \cos(\theta) \end{bmatrix} u.$$

The motion control problem which we will pose for this system is that for any two points  $x_1 < x_2$  on the track, if the system begins at the point  $x_1$ , it will then eventually pass through the point  $x_2$ . We do not impose a specific timing for this manoeuvre, nor do we prescribe a specific speed for the cart, but we do require the speed to be bounded. Further, we want this manoeuvre to be performed without any excessive “swinging” of the payload, and therefore we want to design a regular VHC such that the angle  $\theta$  stays in a specified interval  $[-\theta_{\max}, \theta_{\max}]$ . We call this a *geometric specification*. Additionally, we want all orbits of the constrained dynamics carry the system from  $x_1$  to  $x_2$ , for all  $x_1 < x_2$ . We call this a *dynamic specification*.

## 4.2 Cart-acrobot

The second example we consider is the *cart-acrobot*, illustrated in Figure 2b, a double pendulum mounted on a cart. The cart-acrobot has three degrees of freedom and two actuators: a force applied to the cart, and a torque applied at the second joint of the double pendulum. We suppose that at some position along the track there is located an overhead obstacle, as depicted in Figure 2b. Let  $x$  be the position of the cart along the track,  $\theta_1$  the angle of the first link relative to the vertical, and  $\theta_2$  the angle of the second link relative to the first, both measured counterclockwise. Let  $l_1$  and  $l_2$  be the lengths of the first and second link respectively. The equations of motion for the system have the standard form (2), where the entries of the mass matrix  $D$  are

$$\begin{aligned} D_{11} &= M + m_1 + m_2 \\ D_{12} &= -l_1(m_1 + m_2) \cos(\theta_1) - l_2 m_2 \cos(\theta_1 + \theta_2) \\ D_{13} &= -l_2 m_2 \cos(\theta_1 + \theta_2) \\ D_{22} &= m_1 l_1^2 + m_2(l_1^2 + 2l_1 l_2 \cos(\theta_2) + l_2^2) \\ D_{23} &= m_2 l_2^2 + m_2 l_1 l_2 \cos(\theta_2) \\ D_{33} &= m_2 l_2^2 \end{aligned}$$

the potential  $P(q) = m_1 g l_1 \cos(\theta_1) + m_2 g (l_1 \cos(\theta_1) + l_2 \cos(\theta_1 + \theta_2))$ , and the input matrix is  $B(q) = [\mathbf{e}_1 \ \mathbf{e}_3]$ . A smooth left annihilator for  $B(q)$  is  $(B^\perp(q))^\top = -\mathbf{e}_2$ . Using  $(B^\perp)^\top$  for  $f$ , and  $\text{adj}(D(q))B(q)$  for  $g$ , the VCG is

$$\frac{dq}{ds} = -\mathbf{e}_2 + g_1 u_1 + g_2 u_2 \quad (17)$$

where  $g_1$  and  $g_2$  are the columns of  $g$ , suppressed here for space.

The high-level motion control objective for the cart-acrobot is to make it execute a periodic motion, while avoiding the overhead obstacle. Within the framework of this paper, this reduces to designing a regular VHC such that the constraint avoids the obstacle set (the geometric specification), and that the constrained dynamics of the VHC contain periodic orbits around a specified point (the dynamic specification).

The two examples outlined above illustrate two kinds of dynamic specifications for the constrained dynamics arising from a VHC. The first kind, appearing in the overhead crane example, requires solutions of the constrained dynamics to traverse the entire VHC curve in one direction. The second kind, appearing in the cart-acrobot example, requires all solutions of the constrained dynamics to be periodic. In the next section we formalize these two specifications and show how to transform them into control specifications for the VCG.

## 5 The Dynamic Problem

In this section we address the following *dynamic problem*: design a regular VHC such that the solutions of the constrained dynamics (5) have certain qualitative properties. Motivated by the two foregoing examples, we focus on the properties presented in the next two problems.

**Dynamic Problem 1** (DP1, VHCs for traversal). Design a parametric VHC  $\sigma : \mathbb{R} \rightarrow \mathcal{Q}$  for system (2) such that, for all initial conditions  $(s(0), \dot{s}(0))$  of the resulting constrained dynamics (5), the following properties hold:

- (1)  $s(t) \rightarrow \infty$  as  $t \rightarrow \infty$ , and
- (2)  $(\exists a > 0)(\forall t \in \mathbb{R}) \left\| \frac{d}{dt} \sigma(s(t)) \right\| \leq a$ .

The first condition guarantees that for any points  $s_1 < s_2$ , any solution starting at  $s_1$  eventually passes through  $s_2$ . The second condition encodes that this occurs with bounded speed in the configuration space of the robot.

The second dynamic problem arises when we want to design constraints achieving a repetitive motion. We begin by defining what constitutes a repetitive motion for the constrained dynamics (5). Let  $s^* \in \mathbb{R}$ . We will say that an orbit of the constrained dynamics (5) is an *oscillation around  $s^*$*  if it is either a closed orbit encircling the point  $(s^*, 0)$ , or an equilibrium at  $(s^*, 0)$ . Achieving a repetitive motion then amounts to designing a constraint whose orbits are oscillations.

**Dynamic Problem 2** (DP2, VHCs for oscillations). Design a parametric VHC  $\sigma : \mathbb{R} \rightarrow \mathcal{Q}$  for (2) such that all orbits of the constrained dynamics (5) are oscillations.

In Propositions 5 and 7 of Section 5.1 we show that the requirements of DP1 and DP2 amount to requirements on the function  $\Psi_1(s)$  appearing in the constrained dynamics (5). In Section 5.2 we will show that  $\Psi_1(s)$  can be viewed as an output signal of the VCG, and using this insight we will convert the two dynamic problems into control specifications for the VCG, which in turn will inform the formulation of an optimal control problem in Section 6.

### 5.1 Conditions on $\Psi_1(s)$ solving DP1 and DP2

Recall from Section 2 that all constraints that are open curves have constrained dynamics which are Euler-Lagrange with one degree of freedom. In order to take advantage of this fact, we will restrict our attention to open-curve constraints in everything that follows.

To gain intuition about our problems, suppose for a moment that the virtual mass  $M(s) \equiv 1$ . Then the constrained dynamics (5) simplify to  $\ddot{s} = -V'(s) = \Psi_1(s)$ ,

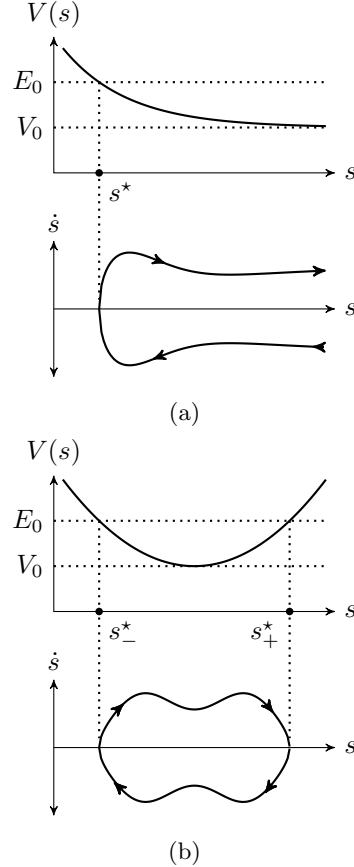


Fig. 3. E-L dynamics for the two classes of desired motions. For traversal, shown in (a), the potential should be unbounded above, to prevent escape in the wrong direction, strictly decreasing, so that the system accelerates in the correct direction, and bounded below, so that the kinetic energy, and therefore the speed, is bounded. For oscillations, in (b), the potential should grow without bound in both directions away from the centre of oscillation, located at the minimum of the potential energy, so that the particle is trapped in the potential well.

and as is well known from classical mechanics, all important qualitative properties of the solutions can be deduced from the potential  $V$ . Oscillations around  $s^*$  occur when  $V$  is convex and has a global minimum at  $s^*$ , while traversal occurs when the potential is monotonically decreasing and unbounded above. Bounded speed is guaranteed by the potential being bounded below. See Figure 3 for an illustration of these properties. Since  $V'(s) = -\Psi_1(s)$ , for DP1 the properties just stated translate directly into these requirements on  $\Psi_1$ :

$$\Psi_1 > 0, \int_0^\infty \Psi_1(\tau) d\tau < \infty, \int_0^{-\infty} \Psi_1(\tau) d\tau = -\infty. \quad (18)$$

The question now is whether the intuition just developed is still valid when the virtual mass  $M(s)$  is not constant. The answer is yes, to a large extent.

**Proposition 5** (Conditions for DP1). *For the constrained dynamics in (5), suppose that the function  $\Psi_1(s)$  satisfies the requirements in (18), and that there exist two positive constants  $M_1, M_2$  such that the function  $M(s)$  in (9a) satisfies  $0 < M_1 < M(s) < M_2$  for all  $s \in \mathbb{R}$ . Then, for each initial condition  $(s(0), \dot{s}(0)) = (s_0, \dot{s}_0) \in \mathbb{R} \times \mathbb{R}$  of the constrained dynamics (5),  $s(t) \rightarrow \infty$  and  $\dot{s}(t)$  is bounded. If, in addition,  $\sigma(s)$  is a solution of the VCG (11) with a bounded virtual control signal  $\bar{u} : \mathbb{R} \rightarrow \mathbb{R}^{n-1}$ , and there exists  $A > 0$  such that  $\|f(q)\|, \|g(q)\| < A$  for all  $q \in \mathcal{Q}$ , then  $\sigma'(s(t))\dot{s}(t)$  is also bounded, and DP1 is solved.*

**Remark 6.** There is no loss of generality in the assumption that  $\|f\|, \|g\| < A$ , for if the VCG fails to satisfy it, we may replace  $f$  and  $g$  by their normalized counterparts, and Proposition 3 implies that the resulting control system is still a VCG, now satisfying the required properties. The value of the constant  $A$  does not need to be known.

*Proof.* By definition,  $V(s) = -\int_0^s \Psi_1(\tau)M(\tau) d\tau$ . Since both  $M$  and  $\Psi_1$  are strictly greater than zero,  $V$  is strictly decreasing. Since  $M(s)$  is bounded above by  $M_2$ , for all  $s \geq 0$  we have  $V(s) \geq -M_2 \int_0^s \Psi_1(\tau) d\tau$ . By assumption,  $\int_0^\infty \Psi_1(\tau) d\tau < \infty$ , implying that  $\liminf_{s \rightarrow \infty} V(s) > -\infty$ . Since  $V$  is strictly decreasing,  $V$  is bounded from below, and therefore it has a limit  $\lim_{s \rightarrow \infty} V(s) = V_0$ . Similarly, for all  $s \leq 0$  we have  $V(s) \geq -M_1 \int_0^s \Psi_1(\tau) d\tau$ . Since, by assumption,  $\int_0^{-\infty} \Psi_1(\tau) d\tau = -\infty$ , we deduce that  $V(s) \rightarrow \infty$  as  $s \rightarrow -\infty$ .

Given an initial condition  $(s(0), \dot{s}(0)) = (s_0, \dot{s}_0)$  for the constrained dynamics (5), the solution  $(s(t), \dot{s}(t))$  lies on the energy level set

$$E_{e_0} := \{(s, \dot{s}) : E(s, \dot{s}) = (1/2)M(s)\dot{s}^2 + V(s) = e_0\},$$

where  $e_0 = E(s_0, \dot{s}_0)$ . Since the energy function  $E(s, \dot{s})$  is a first integral of the constrained dynamics (5), the level set  $E_{e_0}$  is invariant for (5). We claim that in fact  $E_{e_0}$  is an orbit of (5). First off, since  $V$  is monotonically decreasing and its image is the open interval  $V(\mathbb{R}) = (V_0, \infty)$ ,  $V$  has a  $C^1$  inverse  $V^{-1} : (V_0, \infty) \rightarrow \mathbb{R}$ . Let  $I_{e_0} = (-\sqrt{2(e_0 - V_0)}, \sqrt{2(e_0 - V_0)})$  and define the map  $\gamma : I_{e_0} \rightarrow E_{e_0}$  as

$$\begin{aligned} (s, \dot{s}) &= \gamma(\theta) \\ &= (V^{-1}(e_0 - \theta^2/2), \theta/\sqrt{M \circ V^{-1}(e_0 - \theta^2/2)}). \end{aligned}$$

The map  $\gamma$  is a diffeomorphism with inverse  $\gamma^{-1} : E_{e_0} \rightarrow I_{e_0}$ ,  $(s, \dot{s}) \mapsto \theta = \sqrt{M(s)}\dot{s}$ , and thus the level set  $E_{e_0}$  is a curve diffeomorphic to the real line. On this level set, the constrained dynamics have no equilibria since  $V'(s) \neq 0$ , which implies that the invariant curve  $E_{e_0}$  is

an orbit of (5), as claimed. The bottom half of Figure 3a depicts a typical such orbit.

Having established that the level set  $E_{e_0}$  is an orbit of (5), we now show that the solution  $(s(t), \dot{s}(t))$  satisfies  $s(t) \rightarrow \infty$  as  $t \rightarrow \infty$  and  $|\dot{s}(t)|$  is bounded. To this end, from the parametrization  $\gamma(\theta)$  of  $E_{e_0}$  we deduce that the projection of  $E_{e_0}$  onto the  $s$ -axis is the interval  $(V^{-1}(e_0), \infty)$  which, since  $E_{e_0}$  is an orbit of (5), implies that  $s(t) \rightarrow \infty$ . Finally, the identity  $E(s, \dot{s}) = e_0$  implies that

$$\dot{s}^2 = \frac{2(e_0 - V(s))}{M(s)} \leq \frac{2(e_0 - V_0)}{m}.$$

Thus  $|\dot{s}(t)|$  is bounded along the orbit.

Finally, if  $\sigma(s)$  is a solution of the VCG for a bounded virtual control signal  $\bar{u}(s)$ , we have  $\sigma'(s) = f(\sigma(s)) + g(\sigma(s))\bar{u}(s)$ . Since  $\sigma'(s)$  is a sum of bounded terms, there exists  $C > 0$  such that for each  $s \in \mathbb{R}$ ,  $\|\sigma'(s)\| < C$ . So  $\|\sigma'(s)\dot{s}(t)\|$  is bounded, and the proposition is proved.  $\square$

Now we turn to DP2.

**Proposition 7** (Conditions for DP2). *For the constrained dynamics in (5), let  $s^* \in I \subseteq \mathbb{R}$  be such that  $\Psi_1(s^*) = 0$ , and  $(s - s^*)\Psi_1(s) < 0$  for all  $s \in I, s \neq s^*$ . Then there exists a neighbourhood of  $(s^*, 0) \in \mathbb{R}^2$  such that all solutions of (5) with initial conditions from that neighbourhood are oscillations. Further, suppose that  $I = \mathbb{R}$ ,  $\int_0^{\pm\infty} \Psi_1(\tau) d\tau = \infty$ , and that there exists a positive constant  $M_1$  such that  $M(s) > M_1 > 0$  for all  $s \in \mathbb{R}$ . Then, all solutions of (5) are oscillations around  $s^*$ , and DP2 is solved.*

*Proof.* The result is a simple extension of Theorem 3 in [26]. Also see Propositions 8 and 9 in [23].  $\square$

**Remark 8.** The conditions of the preceding two propositions clearly cannot be satisfied if  $\nabla P$  is everywhere in  $\ker(B^\perp)$ . In particular, if the potential is constant, then the conditions cannot be satisfied.

## 5.2 Control specifications for the VCG

We now have specific requirements for  $\Psi_1$  solving DP1 and DP2. It only remains to encode these requirements in a control specification for the VCG. The key observation is that we can view  $\Psi_1$  as an output signal of the VCG, where the output function is<sup>3</sup>

$$\tilde{\Psi}_1(q) = -\frac{B^\perp(q)\nabla P(q)}{B^\perp(q)D(q)f(q)}. \quad (19)$$

<sup>3</sup> The defining property (12) of the VCG and the fact that  $\text{Ker } B^\perp = \text{Im } B$  imply that the denominator of  $\tilde{\Psi}_1$  is nonzero, and thus  $\tilde{\Psi}_1 : \mathcal{Q} \rightarrow \mathbb{R}$  is smooth.

To see that this is the case, recall that by (6) we have

$$\Psi_1(s) = - \frac{B^\perp \nabla P}{B^\perp D \sigma'(s)} \Big|_{q=\sigma(s)}.$$

Substitution of the VCG dynamics (11) for  $\sigma'(s)$  in the denominator yields

$$B^\perp(\sigma(s))D(\sigma(s))(f(\sigma(s)) + g(\sigma(s))u(s)).$$

Since  $\text{Im}(g(q)) = \text{Im}(D^{-1}(q)B(q))$ , which is exactly the kernel of  $B^\perp(q)D(q)$ , this reduces to

$$B^\perp(\sigma(s))D(\sigma(s))f(\sigma(s)),$$

which is exactly  $\tilde{\Psi}_1 \circ \sigma$ . So, we consider the VCG *with output*

$$\begin{aligned} \frac{dq}{ds} &= f(q) + g(q)u \\ e &= \tilde{\Psi}_1(q). \end{aligned} \quad (20)$$

Using the above, we can now reframe our two dynamic problems as control specifications for the VCG. Consider the VCG with output (20), where  $\tilde{\Psi}_1$  is given in (19). Fix an initial condition  $q_0$  and consider the following control specifications:

**SPEC 1.** Find a virtual control signal  $u : \mathbb{R} \rightarrow \mathbb{R}^{n-1}$  such that the corresponding output signal  $\tilde{\Psi}_1(\sigma(s))$  satisfies  $\tilde{\Psi}_1(\sigma(s)) > 0$ ,  $\int_0^\infty \tilde{\Psi}_1(\sigma(s)) ds < \infty$ , and  $\int_{-\infty}^0 \tilde{\Psi}_1(\sigma(s)) ds = \infty$ .

**SPEC 2.** Find a virtual control signal  $u : \mathbb{R} \rightarrow \mathbb{R}^{n-1}$  such that the corresponding output signal  $\tilde{\Psi}_1(\sigma(s))$  satisfies  $\tilde{\Psi}_1(\sigma(s^*)) = 0$  for some  $s^* \in \mathbb{R}$ , and  $\tilde{\Psi}_1(\sigma(s))$  is strictly decreasing.

By Propositions 5 and 7, a controller for the VCG meeting SPEC 1 and yielding a virtual mass that is bounded away from zero and bounded from above gives a parametric VHC solving DP1<sup>4</sup>, while one meeting SPEC 2 and yielding a virtual mass that is bounded away from zero gives a parametric VHC solving DP2.

The requirements on the boundedness of  $M(s)$  are not explicitly stated in SPEC 1 and SPEC 2. While it is not difficult to incorporate them into the optimal control formulation we present in the next section, the requirements only concern the properties of  $M(s)$  in the limit  $s \rightarrow \pm\infty$ , and the computational procedure that we use only generates the constraint over a finite interval of the parameter  $s$ .

<sup>4</sup> Provided that the functions  $f$  and  $g$  appearing in the VCG are chosen to be uniformly bounded. By Proposition 3, this can always be done through normalization.

**Remark 9.** It is not hard to find feedback controllers for the VCG meeting SPEC 1 and SPEC 2, and this was done in [22]. These controllers, however, rely on unnecessarily strong assumptions and make it hard to address geometric specifications. In the following section, we will develop an optimal control formulation of the constraint planning problem which, in addition to encompassing various geometric specifications for the VHCs, cleanly incorporates the necessary requirements for  $\tilde{\Psi}_1$  so that a constraint solving the total constraint planning problem emerges as the solution of a single optimal control problem for the VCG, and in such a way that a solution may be found even when the conditions of [22] are not satisfied.

## 6 Synthesis of constraints through optimal control

By Theorem 2, the solutions of the VCG (11) constitute all possible parametric VHCs for the mechanical system (2), up to reparametrization. In light of this result, the constraint design problem described in the introduction amounts to a search over the solution space of the VCG, subject to the constraints imposed by the geometric and dynamic specifications. In this section we formulate this search as an optimal control problem of this form:

$$\text{minimize}_{u \in \mathcal{U}} \int_{\sigma(\mathbb{R})} G(q, u) dq \quad (21a)$$

$$\text{subject to } \sigma'(s) = f(\sigma(s)) + g(\sigma(s))u(s) \quad (21b)$$

$$\zeta_0(\sigma(0)) = 0 \quad (21c)$$

$$\zeta_1(\sigma(T)) = 0 \quad (21d)$$

$$\eta_j(s, \sigma(s), u(s)) \leq 0, \quad j \in \{1, \dots, k\}. \quad (21e)$$

In the above,  $\mathcal{U}$  is the set of admissible virtual control signals for the VCG, that is, the set of  $C^1$  functions  $u : \mathbb{R} \rightarrow \mathbb{R}^{n-1}$ . The differential equation (21b) is the VCG, and it is the feature guaranteeing that the optimization is performed over the set of all possible regular VHCs. The function  $G : \mathcal{Q} \times \mathbb{R}^{n-1} \rightarrow \mathbb{R}$  is the instantaneous cost, and the objective function is the path integral of  $G$  along a solution of the VCG. The equality constraints (21c) and (21d) impose requirements on the initial condition of the VCG and the terminal value of the solution at some time  $T > 0$ , where  $T$  is either fixed or variable. If there are none such requirements, we simply set  $\zeta_0$  or  $\zeta_1$  equal to zero. Finally, the inequality constraints in (21e) encode both geometric and dynamic specifications. In what follows, we discuss these ingredients in more detail.

*The instantaneous cost.* The objective function is the path integral of the instantaneous cost along a solution  $\sigma(s)$  of the VCG. The integral in question is defined as

$$\int_{\sigma(\mathbb{R})} G(q, u) dq = \int_{\mathbb{R}} G(\sigma(s), u(s)) \|\sigma'(s)\| ds.$$

The function  $G$  can be chosen to reduce actuator usage along a specific orbit of the constrained dynamics, or to encode geometric features of the VHC curve. For instance, if we wanted to find a minimum-length VHC curve we would set  $G \equiv 1$ . In the cart-acrobot example presented in Section 8 below, we use  $G$  to penalize states where the acrobot is excessively “crouched,” whereas for the crane example of Section 7 we choose  $G$  to induce the greatest possible cumulative acceleration along the track.

*Equality constraints.* The equality constraint (21c) can be used to express requirements on the initial condition of the VCG arising from the dynamic problem. Specifically, we have seen in Section 5.2 that when it comes to inducing oscillations in the constrained dynamics, SPEC 2 requires  $\tilde{\Psi}_1(\sigma(s^*)) = 0$ . Without loss of generality, we may assume  $s^* = 0$  and set  $\zeta_0 = \tilde{\Psi}_1$  in (21c). To meet SPEC 1 (traversal), on the other hand, there are no requirements on the initial condition so we set  $\eta_0 \equiv 0$ . The constraint (21d) can be used to impose that the VHC curve reaches the zero level set of  $\zeta_1$ . In a typical scenario, we might want the VHC curve to connect two points  $q_0, q_1 \in \mathcal{Q}$ , in which case we could set  $\zeta_0(\sigma(0)) = \sigma(0) - q_0$  and  $\zeta_1(\sigma(T)) = \sigma(T) - q_1$ .

*Inequality constraints.* The inequality constraints in (21e) arise from both the geometric and dynamic specifications. A typical geometric specification is obstacle avoidance. Let the safe set  $\mathcal{S} \subset \mathcal{Q}$  represent the subset of the configuration space where the robot does not intersect with obstacles in the task space. Representing the safe set as the sublevel set of a function  $\eta : \mathcal{Q} \rightarrow \mathbb{R}^l$ ,  $\mathcal{S} = \{q \in \mathcal{Q} : \eta(q) \leq 0\}$  (where the inequality is to be understood component-wise), the obstacle avoidance requirement can be written as  $\eta(\sigma(s)) \leq 0$ , which fits the form in (21e).

Another geometric requirement is *monotonicity* of certain quantities along the VHC curve. To illustrate, consider the overhead crane example, and suppose we want to make the trolley traverse to the end of the track. Designing a constraint meeting the conditions of DP1 is not sufficient, because an increase in  $s$  does not guarantee that the trolley moves along the track; it is possible that increasing  $s$  could correspond to the trolley backtracking, or even a change in the swing angle without any corresponding motion of the trolley at all. We formalize this requirement by imposing that a function  $\mu : \mathcal{Q} \rightarrow \mathbb{R}$  be monotonic along solutions of the VCG, without loss of generality decreasing. In other words, we require that the function  $s \mapsto \mu \circ \sigma(s)$  be monotonically decreasing. In the case of the crane,  $\mu$  would be the function extracting the track position from the state  $q$ . Using the fact that  $\sigma(s)$  is a solution of the VCG, and requiring the derivative of  $\mu \circ \sigma(s)$  to be nonpositive, the monotonicity requirement gives the inequality constraint

$$-d\mu_{\sigma(s)}(f(\sigma(s)) + g(\sigma(s))u(s)) \leq 0, \quad (22)$$

which has the form of the general inequality constraint in (21e).

Now we turn to the dynamic problems DP1 and DP2, which in Section 5.2 were converted into two sets of control specifications of the VCG, SPEC 1 and SPEC 2, respectively. These specifications are easily seen to amount to inequality constraints of the form (21e). SPEC 2 for oscillations requires a constraint  $q = \sigma(s)$  with the property that the function  $s \mapsto \tilde{\Psi}_1(\sigma(s))$  is decreasing and that  $\tilde{\Psi}_1(\sigma(s^*)) = 0$ . We have already included the latter equality constraint in (21c). The remaining requirement can be expressed as an inequality constraint for the derivative

$$(d\tilde{\Psi}_1)_{\sigma(s)}(f(\sigma(s)) + g(\sigma(s))u(s)) + \varepsilon \leq 0, \quad (23)$$

where  $\varepsilon > 0$  is a small design parameter. The constraint (23) has once again the form (21e).

For meeting SPEC 1 for traversal, we take a similar approach. The first requirement of the control specification is simply that  $\tilde{\Psi}_1(\sigma(s)) > 0$ , which can be expressed as  $-\tilde{\Psi}_1(\sigma(s)) + \varepsilon \leq 0$ , with  $\varepsilon > 0$  a small design parameter. The next requirement is to achieve the convergence of  $\int_0^\infty \tilde{\Psi}_1(\sigma(s)) ds$ . For this, we impose a differential inequality

$$\begin{aligned} \frac{d}{ds} \tilde{\Psi}_1(\sigma(s)) &= d(\tilde{\Psi}_1)_{\sigma(s)}(f(\sigma(s)) + g(\sigma(s))u(s)) \\ &\leq \beta(s, \tilde{\Psi}_1(\sigma(s))), \end{aligned} \quad (24)$$

where  $\beta$  is any function such that the solutions of the differential equation  $\dot{x} = \beta(t, x)$  converge to zero and have finite  $L_1$  norm on  $[0, \infty)$ . The simplest such choice would be  $\dot{x} = -x$ . This gives a constraint of the form (21e). The final requirement of SPEC 1 is the divergence of  $\int_{-\infty}^0 \tilde{\Psi}_1(\sigma(s)) ds$ , which can be achieved by an inequality bounding  $\tilde{\Psi}_1(\sigma(s))$  below by a positive constant for  $s < 0$ .

## 7 Example 1: the overhead crane

We now return to the overhead crane example and formulate an optimal control problem of the form (21) to synthesize a VHC making the trolley move from any initial point  $x_1 \in \mathbb{R}$  to any final point  $x_2 > x_1$  with bounded speed, while keeping the cable angle  $\theta$  confined within the interval  $[-\theta_{\max}, \theta_{\max}]$ . This latter requirement amounts to having a safe set  $\mathcal{S} = \{q \in \mathcal{Q} : |\theta| \leq \theta_{\max}\}$  which gives our first inequality constraint. Next, we have the monotonicity requirement to make the trolley traverse the track along the VHC curve. For this, we set  $\mu(q) = x$  and get the inequality constraint in (22), which reduces to  $ml^2u(s) \geq 0$ , or equivalently  $-u(s) \leq 0$ . Finally, we have inequality constraints in order to meet SPEC 1 for traversal. We will address the

convergence inequality (24) first. For this system,  $\tilde{\Psi}_1$  computed using (19), is  $\tilde{\Psi}_1(q) = (g/l) \sin(\theta)$ , and so we have the inequality

$$\frac{g}{l} \cos(\theta)(-1 + ml \cos(\theta)u) \leq -\frac{g}{l} \sin(\theta),$$

where we have used  $\beta(s, \tilde{\Psi}_1(s)) = -\tilde{\Psi}_1(s)$ . This ensures the convergence of  $\int_0^\infty \tilde{\Psi}_1(\sigma(s)) ds$ . Both the divergence of  $\int_{-\infty}^0 \tilde{\Psi}_1(s) ds$  and the strict positivity of  $\tilde{\Psi}_1(\sigma(s))$  are enforced by the inequality  $\tilde{\Psi}_1(\sigma(s)) \geq \varepsilon/(1 + e^s)$ , for some  $\varepsilon > 0$ .

Finally, we discuss the instantaneous cost. For this problem, so long as the swing angle of the payload remains within the safe limits, and the desired dynamic behaviour is achieved by the constraint, any configuration of the system is equally preferable. We are, however, interested in achieving a fast motion along the track. So, we select  $G(q) = -\tilde{\Psi}_1(q)$ , so that the constraints we design induce the greatest possible cumulative acceleration along the track, subject to our other requirements. This leaves us with the optimal control problem

$$\begin{aligned} \text{minimize} \quad & \int_{\mathbb{R}} -\frac{g}{l} \sin(\sigma_2(s)) \|\sigma'(s)\| ds \\ \text{subject to} \quad & \sigma'(s) = \begin{bmatrix} 0 \\ -1 \end{bmatrix} + \begin{bmatrix} ml^2 \\ ml \cos(\sigma_2(s)) \end{bmatrix} u(s), \\ & -u(s) \leq 0, \\ & |\sigma_2(s)| \leq \theta_{\max}, \\ & -\tilde{\Psi}_1(\sigma(s)) + \frac{\varepsilon}{1 + e^s} \leq 0, \\ & \frac{g}{l} \cos(\sigma_2(s))(-1 + ml \cos(\sigma_2(s))u(s)) \\ & \quad + \frac{g}{l} \sin(\sigma_2(s)) \leq 0. \end{aligned}$$

Figure 4 shows the constraint generated according to the above requirements. We note some of the key features of this constraint to provide some intuition on how it meets these requirements. Starting on the left, we note that the payload starts off with a negative swing angle. Since the payload is unactuated, in order for the controller to maintain this angle under the influence of gravity, the trolley has to accelerate towards the right. As we proceed along the constraint in this direction, the swing angle of the payload begins to decrease, until it hangs vertically at the right end of the constraint. Now in order for the controller to maintain this vertical angle, the trolley has to move at a constant (bounded) speed, meeting our requirement for traversal. We note that the constraint just designed is very simple, and the intuitive considerations just outlined could have been used to design this constraint without any of the mathematical formalism we have developed. This constraint,

however, shows that our procedure produces reasonable constraints which would be expected to solve the desired problem. In the following section we will design a more complicated constraint, which would not be so easy to design simply from intuition.

Now a final comment about the constraint designed above. At the ‘‘end’’ of its motion along this constraint, the trolley is moving at some constant speed, while the payload hangs vertically. For practical applications, the trolley must of course be brought to a stop. Achieving this behaviour is the topic of a future paper.

## 8 Example 2: the cart-acrobot

Returning to the cart-acrobot example, we recall that the objective is to make the robot perform a repetitive back-and-forth motion underneath the obstacle. We will model our obstacle as a circular obstruction at a height  $h$  above the central  $x = 0$  position of the track, with radius  $r$ . The safe set is then given by two inequality constraints,  $\eta_1(q) \leq 0$  and  $\eta_2(q) \leq 0$ , with

$$\begin{aligned} -\eta_1(q) &= (x - l_1 \sin(\theta_1))^2 + (h - l_1 \cos(\theta_1))^2 - r^2, \\ -\eta_2(q) &= (x - l_1 \sin(\theta_1) - l_2 \sin(\theta_1 + \theta_2))^2 \\ &\quad + (h - l_1 \cos(\theta_1) - l_2 \cos(\theta_1 + \theta_2))^2 - r^2. \end{aligned}$$

Since we want the dynamic back-and-forth motion to happen along the track, we impose a monotonicity constraint by setting  $\mu(q) = x$ . In this case, the inequality constraint (22) reduces to

$$-g_{1,1}(\sigma(s))u_1(s) - g_{2,1}(\sigma(s))u_2(s) \leq 0.$$

Next we turn to the dynamic requirements, which in this case fit the formulation of DP2 because we want the cart to perform a repetitive motion underneath the obstacle. We want the oscillations of the constrained dynamics to be centred around the  $x = 0$  position. To this end, we set the first component of  $\sigma(0)$  (the  $x$ -component) to zero, and following SPEC 2 we require  $\tilde{\Psi}_1(\sigma(0)) = 0$ . Next, we impose the inequality constraint (23) (we omit its expression since it is quite complicated).

Finally, for the instantaneous cost, we want to penalize positions which are away from the upright position, so we choose

$$G(q) = \alpha\theta_1^2 + \beta\theta_2^2.$$

Assembling all this together, we have the optimal control

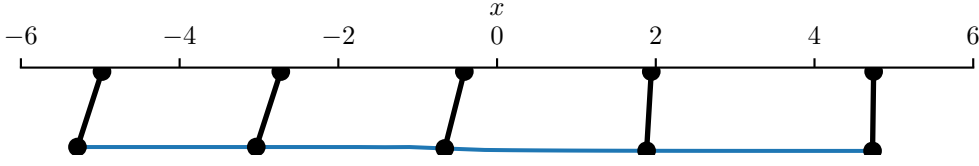


Fig. 4. The generated constraint for the overhead crane

problem

$$\begin{aligned}
& \underset{u \in \mathcal{U}}{\text{minimize}} && \int_{\mathbb{R}} (\alpha \theta_1^2(s) + \beta \theta_2^2(s)) \|\sigma'(s)\| ds \\
& \text{subject to} && \sigma'(s) = f(\sigma(s)) + g(\sigma(s))u(s), \\
& && \sigma_1(0) = 0, \\
& && \tilde{\Psi}_1(\sigma(0)) = 0, \\
& && -(x - l_1 \sin(\sigma_2(s)))^2 \\
& && \quad - (h - l_1 \cos(\sigma_3(s)))^2 + r^2 \leq 0, \\
& && -(x - l_1 \sin(\sigma_2(s)) - l_2 \sin(\sigma_2(s) + \sigma_3(s)))^2 \\
& && \quad - (h - l_1 \cos(\sigma_2(s)) - l_2 \cos(\sigma_2(s) + \sigma_3(s)))^2 \\
& && \quad \quad \quad + r^2 \leq 0, \\
& && -g_{1,1}(\sigma(s))u_1(s) - g_{2,1}(\sigma(s))u(s) \leq 0, \\
& && d(\tilde{\Psi}_1)_{\sigma(s)}(f(\sigma(s)) + g(\sigma(s))u(s)) \leq 0.
\end{aligned}$$

We solve this problem numerically using direct collocation. The resulting constraint is shown in Figure 5. As in the previous example, we can derive some insight into this constraint with some simple examination. Starting at the left, we can see that the cart-acrobot is nearly upright, with the middle “elbow” joint pushed out to the right. As a result of this, the centre-of-mass of the system is displaced right of the base. To maintain this position, the cart must accelerate to the right. As we approach the centre of the track and the obstacle, the acrobot takes on a more crouched pose to pass under the obstacle, remaining as extended as possible to minimize the cost, while not violating the obstacle avoidance constraint. Moving to the right, the top of the acrobot just maintains contact with the edge of the obstacle set. At the centre of the track, the centre-of-mass of the acrobot is directly over the base, so that  $\tilde{\Psi}_1$  is zero. Once past the obstacle, it continues to straighten up, passing through a kinematic singularity so that the middle joint is pushed out to the left, mirroring the pose at the left of the track, and similarly displacing the centre-of-mass towards the centre of the track. As on the left, the cart must accelerate towards the centre of the track to maintain this pose, leading to the desired oscillatory behaviour.

A dynamic simulation of the cart-acrobot system was conducted, with the constraint enforced using the controller from [18]. Figure 6 shows the results of this simulation for the  $x$  and  $\dot{x}$  components. The system was initialized off of the constraint. The controller quickly

drives the cart-acrobot to the constraint, and it subsequently adopts the oscillatory behaviour induced by the constraint, stably oscillating around the  $x = 0$  position.

## 9 Conclusions

We have proposed a synthesis via optimal control of regular VHCs meeting both geometric and dynamic specifications. In contrast to most existing methods, our approach does not rely on the use of Bézier polynomials, or the explicit use of the full robot dynamics to design a constraint achieving a motion objective. Most importantly, built into the proposed approach is the property that the VHC curves it produces are regular.

The focus of this paper is the synthesis of regular VHCs satisfying certain properties. Once a VHC has been found, one can either enforce it using input-output linearization as in [18], or simply stabilize one of the orbits on the constraint manifold using transverse linearization as in [29].

The approach we have presented has many open avenues for future work. For example, the application of more advanced motion planning techniques would allow for the design of constraints for systems with complex obstacle sets. How to exploit the techniques described here to design families of constraints for achieving more complex motion control tasks, and how to best integrate techniques to stabilize particular orbits of a constraint, are also important questions to explore.

## A Proofs of Propositions 3 and 4

*Proof of Proposition 3.* First, we show that if (11) is a VCG, then for all smooth functions  $\alpha : \mathcal{Q} \rightarrow \mathbb{R} \setminus \{0\}$ ,  $K_1 : \mathcal{Q} \rightarrow \mathbb{R}^m$  and  $K_2 : \mathcal{Q} \rightarrow \text{GL}(n-1; \mathbb{R})$ , system (15) is also a VCG. Equivalently, letting  $\tilde{f}(q) = \alpha(q)f(q) + g(q)K_1(q)$  and  $\tilde{g}(q) = g(q)K_2(q)$ , we need to show that properties (i) and (ii) presented below Definition 1 hold. Property (i) holds because

$$\begin{bmatrix} \tilde{f} \\ \tilde{g} \end{bmatrix} = \begin{bmatrix} f \\ g \end{bmatrix} \begin{bmatrix} \alpha & 0_{1 \times (n-1)} \\ K_1 & K_2 \end{bmatrix},$$

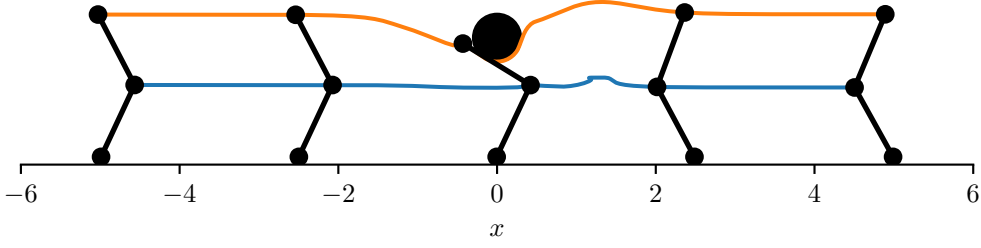


Fig. 5. The generated constraint for the cart-acrobot

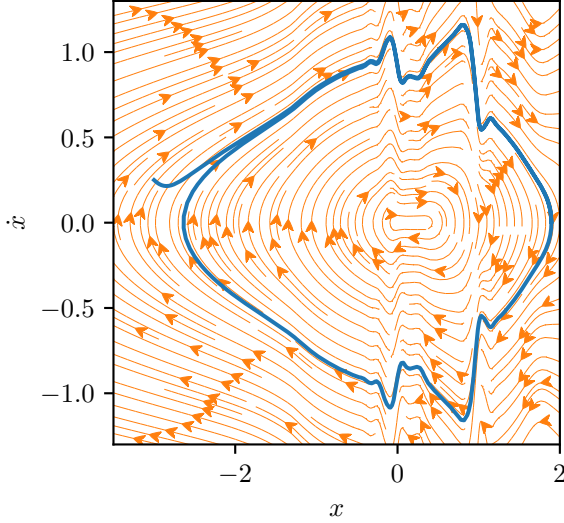


Fig. 6. The  $x$  and  $\dot{x}$  components of a dynamic simulation of the cart-acrobot with a controller enforcing the designed constraint are shown in blue. The cart-acrobot is initialized off the constraint, and the controller drives the system to a stable oscillation around the  $x = 0$  position. In orange are shown the constrained dynamics of the constraint.

and the matrix  $[f \ g]$  is invertible by the assumption that (11) is a VCG, while the second matrix on the right-hand side of the above identity is invertible because  $\alpha \neq 0$  and  $K_2$  is invertible. As for property (ii), we have that

$$\text{Im}(\tilde{g}) = \text{Im}(gK_2) = \text{Im}(g) = \Delta,$$

where the second identity follows from the invertibility of  $K_2$ , while the third identity follows from the fact that (11) is a VCG.

Next, we show that if

$$\frac{dq}{ds} = \tilde{f}(q) + \tilde{g}(q)v \quad (\text{A.1})$$

is a VCG for system (2), then there exist smooth functions  $\alpha : \mathcal{Q} \rightarrow \mathbb{R} \setminus \{0\}$ ,  $K_1 : \mathcal{Q} \rightarrow \mathbb{R}^m$  and  $K_2 : \mathcal{Q} \rightarrow \text{GL}(n-1; \mathbb{R})$  such that  $\tilde{f} = \alpha f + gK_1$  and  $\tilde{g} = gK_2$ . Since both (11) and (A.1) are VCGs, for each  $q \in \mathcal{Q}$  the

matrices  $[f(q) \ g(q)]$  and  $[\tilde{f}(q) \ \tilde{g}(q)]$  are invertible, and thus the matrix

$$M(q) = [f(q) \ g(q)]^{-1} [\tilde{f}(q) \ \tilde{g}(q)]$$

is also invertible. Partitioning  $M(q)$  as follows

$$M(q) = \left[ \begin{array}{c|c} M_{11}(q) & M_{12}(q) \\ \hline M_{21}(q) & M_{22}(q) \end{array} \right],$$

with  $\dim(M_{11}(q)) = 1$  and  $\dim(M_{22}(q)) = (n-1) \times (n-1)$ , we use the fact that (11) and (A.1) are VCGs to deduce that  $\text{Im}(g(q)) = \text{Im}(\tilde{g}(q))$ , which implies that  $M_{12}(q) \equiv 0$ . Now letting  $\alpha(q) = M_{11}(q)$ ,  $K_1(q) = M_{21}(q)$ , and  $K_2(q) = M_{22}(q)$ , we have shown that

$$[\tilde{f} \ \tilde{g}] = [f \ g] M = [f \ g] \begin{bmatrix} \alpha & 0_{1 \times (n-1)} \\ K_1 & K_2 \end{bmatrix},$$

and thus  $\tilde{f} = \alpha f + gK_1$  and  $\tilde{g} = gK_2$ , as required.  $\square$

*Proof of Proposition 4.* By Proposition 3, system (16) is a VCG. Let  $\sigma(s)$  be a solution of the VCG (11) with input signal  $u = \bar{u}(s)$  such that the curve  $q = \sigma(s)$  is a closed embedded submanifold of  $\mathcal{Q}$ . By Theorem 2,  $q = \sigma(s)$  is a parametric VHC. For a reparametrization  $\tilde{\sigma}(\tilde{s}) = \sigma(\mu(\tilde{s}))$ , we have

$$\frac{d\tilde{\sigma}}{d\tilde{s}} = \mu'(\tilde{s})f(\tilde{\sigma}(\tilde{s})) + g(\tilde{\sigma}(\tilde{s}))\bar{u}(\mu(\tilde{s}))\mu'(\tilde{s}). \quad (\text{A.2})$$

Since the set  $\text{Im}(\sigma)$  is a closed embedded submanifold of  $\mathcal{Q}$ , by [17, Lemma 5.34], there exists a smooth function  $\alpha : \mathcal{Q} \rightarrow \mathbb{R}$  such that  $\alpha(\sigma(\tilde{s})) = \mu'(\tilde{s})$ . By definition of reparametrization,  $|\mu'| > \varepsilon > 0$  and so  $|\alpha|_{\sigma(\mathbb{R})} > \varepsilon > 0$ . There is no loss of generality in assuming that  $\alpha \neq 0$  on  $\mathcal{Q}$ , for if it is not, one can use partitions of unity to modify  $\alpha$  outside of  $\sigma(\mathbb{R})$  and guarantee that the resulting function is nonvanishing. With this choice of function  $\alpha$ , from (A.2) we deduce that  $\tilde{\sigma}(\tilde{s})$  is a solution of (16) with virtual control signal  $u = \bar{u}(\mu(\tilde{s}))\mu'(\tilde{s})$ , as claimed.

Next, for each smooth function  $\alpha : \mathcal{Q} \rightarrow \mathbb{R} \setminus \{0\}$ , each solution  $\tilde{\sigma}(\tilde{s})$  of (16) satisfies

$$\tilde{\sigma}'(\tilde{s}) = \alpha(\tilde{\sigma}(\tilde{s}))f(\tilde{\sigma}(\tilde{s})) + g(\tilde{\sigma}(\tilde{s}))\tilde{u}(\tilde{s}), \quad (\text{A.3})$$

for some smooth signal  $\tilde{u} : \mathbb{R} \rightarrow \mathbb{R}^{n-1}$ . Since (16) is a VCG and since  $q = \sigma(s)$  is a parametric VHC, by Theorem 2, there exists a function  $\mu$  such that  $\sigma(\mu(\tilde{s}))$  is a solution of (16), and thus using (A.3) we have

$$\sigma'(\mu(\tilde{s}))\mu'(\tilde{s}) = \alpha(\sigma(\mu(\tilde{s})))f(\sigma(\mu(\tilde{s}))) + g(\sigma(\mu(\tilde{s})))\tilde{u}(\tilde{s}),$$

for some smooth signal  $\tilde{u} : \mathbb{R} \rightarrow \mathbb{R}^{n-1}$ . Since  $\sigma$  is a solution of (11), we can expand the term on the left-hand side to get

$$\begin{aligned} [f(\sigma(\mu(\tilde{s}))) + g(\sigma(\mu(\tilde{s})))\tilde{u}(\mu(\tilde{s}))]\mu'(\tilde{s}) \\ = \alpha(\sigma(\mu(\tilde{s})))f(\sigma(\mu(\tilde{s}))) + g(\sigma(\mu(\tilde{s})))\tilde{u}(\tilde{s}). \end{aligned}$$

Letting  $\tilde{u}(\tilde{s}) = \alpha(\sigma(\mu(\tilde{s})))\tilde{u}(\mu(\tilde{s}))$ , the right-hand side becomes after factoring

$$\alpha(\sigma(\mu(\tilde{s}))) [f(\sigma(\mu(\tilde{s}))) + g(\sigma(\mu(\tilde{s})))\tilde{u}(\mu(\tilde{s}))].$$

Since the bracketed terms are identical, we conclude  $\mu'(\tilde{s}) = \alpha(\sigma(\mu(\tilde{s})))$ , so that  $\mu'(\tilde{s})$  is the unique solution to the differential equation  $x' = \alpha(\sigma(x))$  with initial condition  $x(0) = \mu(0)$ , as claimed.  $\square$

## References

- [1] J.E. Bobrow, S. Dubowsky, and J.S. Gibson. Time-Optimal Control of Robotic Manipulators Along Specified Paths. *The International Journal of Robotics Research*, 4(3):3–17, September 1985.
- [2] Francesco Bullo and Kevin M. Lynch. Kinematic controllability for decoupled trajectory planning in underactuated mechanical systems. *IEEE Transactions on Robotics and Automation*, 17(4):402–412, August 2001.
- [3] C. Chevallereau, G. Abba, Y. Aoustin, F. Plestan, E. R. Westervelt, C. Canudas-de Wit, and J. W. Grizzle. Rabbit: A testbed for advanced control theory. *IEEE Control Systems Magazine*, 23(5):57–79.
- [4] Christine Chevallereau, J. W. Grizzle, and Ching-Long Shih. Asymptotically Stable Walking of a Five-Link Underactuated 3-D Bipedal Robot. *IEEE Transactions on Robotics*, 25(1):37–50, February 2009.
- [5] L. Consolini, A. Costalunga, and M. Maggiore. A coordinate-free theory of virtual holonomic constraints. *Journal of Geometric Mechanics*, 10(4):467–502, 2018.
- [6] L. Consolini and M. Maggiore. Virtual holonomic constraints for Euler-Lagrange systems. In *Symposium on Nonlinear Control Systems (NOLCOS)*, Bologna, Italy, September 2010.
- [7] Luca Consolini, Manfredi Maggiore, Christopher Nielsen, and Mario Tosques. Path following for the PVTOL aircraft. *Automatica*, 46(8):1284–1296, August 2010.
- [8] X. Da, R. Hartley, and J. W. Grizzle. Supervised learning for stabilizing underactuated bipedal robot locomotion, with outdoor experiments on the wave field. In *2017 IEEE International Conference on Robotics and Automation (ICRA)*, pages 3476–3483, May 2017.
- [9] Xingye Da and Jessy Grizzle. Combining trajectory optimization, supervised machine learning, and model structure for mitigating the curse of dimensionality in the control of bipedal robots. *The International Journal of Robotics Research*, 38(9):1063–1097, August 2019.
- [10] Jessy W. Grizzle, Gabriel Abba, and Franck Plestan. Asymptotically stable walking for biped robots: Analysis via systems with impulse effects. *IEEE Transactions on Automatic Control*, 46(1):51–64, 2001.
- [11] J.W. Grizzle, Christine Chevallereau, and Ching-Long Shih. HZD-based control of a five-link underactuated 3D bipedal robot. In *2008 47th IEEE Conference on Decision and Control*, pages 5206–5213, December 2008.
- [12] A. Hereid, E. A. Cousineau, C. M. Hubicki, and A. D. Ames. 3D dynamic walking with underactuated humanoid robots: A direct collocation framework for optimizing hybrid zero dynamics. In *2016 IEEE International Conference on Robotics and Automation (ICRA)*, pages 1447–1454, May 2016.
- [13] A. Hereid, C. M. Hubicki, E. A. Cousineau, and A. D. Ames. Dynamic Humanoid Locomotion: A Scalable Formulation for HZD Gait Optimization. *IEEE Transactions on Robotics*, 34(2):370–387, April 2018.
- [14] A. Hereid, S. Kolathaya, and A. D. Ames. Online optimal gait generation for bipedal walking robots using legendre pseudospectral optimization. In *2016 IEEE 55th Conference on Decision and Control (CDC)*, pages 6173–6179, December 2016.
- [15] John M. Hollerbach. Dynamic Scaling of Manipulator Trajectories. In *1983 American Control Conference*, pages 752–756, June 1983.
- [16] Steven M. LaValle and James J. Kuffner. Randomized Kinodynamic Planning. *The International Journal of Robotics Research*, 20(5):378–400, May 2001.
- [17] J.M. Lee. *Introduction to Smooth Manifolds*. Springer, second edition, 2013.
- [18] M. Maggiore and L. Consolini. Virtual holonomic constraints for Euler-Lagrange systems. *IEEE Transaction on Automatic Control*, 58(4):1001–1008, 2013.
- [19] A. Mohammadi, M. Maggiore, and L. Consolini. On the Lagrangian structure of reduced dynamics under virtual holonomic constraints. *ESAIM: Control, Optimisation and Calculus of Variations*, 23(3):913–935, 2017.
- [20] A. Mohammadi, M. Maggiore, and L. Consolini. Dynamic virtual holonomic constraints for stabilization of closed orbits in underactuated mechanical systems. *Automatica*, 94:112–124, 2018.
- [21] A. Mohammadi, E. Rezapour, M. Maggiore, and K. Y. Pettersen. Maneuvering Control of Planar Snake Robots Using Virtual Holonomic Constraints. *IEEE Transactions on Control Systems Technology*, 24(3):884–899, May 2016.
- [22] Rein Otsason and Manfredi Maggiore. On the Generation of Virtual Holonomic Constraints for Mechanical Systems with Underactuation Degree One. In *58th IEEE Conference on Decision and Control*, 2019.
- [23] Rein Dylan Otsason. *Virtual Constraint Generation*. Thesis, University of Toronto, Toronto, Canada, June 2020.

- [24] F. Pfeiffer and R. Johanni. A concept for manipulator trajectory planning. *IEEE Journal on Robotics and Automation*, 3(2):115–123, April 1987.
- [25] Kang Shin and N. McKay. Minimum-time control of robotic manipulators with geometric path constraints. *IEEE Transactions on Automatic Control*, 30(6):531–541, June 1985.
- [26] A. Shiriaev, A. Robertsson, J. Perram, and A. Sandberg. Periodic motion planning for virtually constrained Euler–Lagrange systems. *Systems & Control Letters*, 55(11):900–907, November 2006.
- [27] A. S. Shiriaev, L. B. Freidovich, A. Robertsson, R. Johansson, and A. Sandberg. Virtual-Holonomic-Constraints-Based Design of Stable Oscillations of Furuta Pendulum: Theory and Experiments. *IEEE Transactions on Robotics*, 23(4):827–832, August 2007.
- [28] Anton S Shiriaev, Leonid B Freidovich, and Sergei V Gusev. Transverse linearization for controlled mechanical systems with several passive degrees of freedom. *IEEE Transactions on Automatic Control*, 55(4):893–906, 2010.
- [29] A.S. Shiriaev, J.W. Perram, and C. Canudas-de-Wit. Constructive tool for orbital stabilization of underactuated nonlinear systems: Virtual constraints approach. *IEEE Trans. Automat. Contr.*, 50(8):1164–1176, August 2005.
- [30] E. R. Westervelt, J. W. Grizzle, and D. E. Koditschek. Hybrid zero dynamics of planar biped walkers. *IEEE Transactions on Automatic Control*, 48(1):42–56, January 2003.
- [31] E.R. Westervelt, C. Chevallereau, J.H. Choi, B. Morris, and J.W. Grizzle. *Feedback control of dynamic bipedal robot locomotion*. CRC press, 2007.
- [32] E.R. Westervelt, J.W. Grizzle, and D.E. Koditschek. Hybrid zero dynamics of planar biped robots. *IEEE Transactions on Automatic Control*, 48(1):42–56, 2003.